

Extending the Calibration of the
ATLAS Hadronic Calorimeter to High P_t

Chris Sears, University of Chicago

May 16th, 2002

Advisor: James Pilcher

Abstract: The ATLAS detector set to run at the CERN LHC in 2007 will study pp collisions with energies of 7 TeV per beam. Many of the interesting physics studies will involve quark and gluon jets with energies of many TeV. To accurately measure such jets, the calorimeter must be calibrated over all energy ranges. This paper presents an overview of calibration techniques, discussing their limitations in obtaining the goal of a full range absolute energy calibration. The γ -jet calibration method discussed shows sufficient statistics for a calibration to energies of roughly 650 GeV in the region with $|\eta|<1$. Also discussed is a possible method for extending individual cell calibration into the TeV range using multi-jet (>2) events.

Introduction

Since the events measured in the ATLAS detector involve collisions of protons, a vast majority of events will involve quarks and gluons in the final state. To study the physics of the interactions during the event, the energy and direction of the final state particles are measured. It is the job of the hadronic calorimeter to measure the energy of quarks and gluons (which hadronize to form jets) from the final state of the event. With this energy measurement and other information gathered from others parts of the ATLAS detector the event can be reconstructed, missing momentum quantified, intermediate particles inferred. With the very high statistics produced by the collider cross-sections are measured and further physics phenomena such as quark compositeness or graviton emission can be studied.

The full calorimeter of the ATLAS detector is broken up into many parts (see fig. 1). Close to the beam line is the electromagnetic calorimeter, which measures the energy of electromagnetically interacting particles, namely photons and electrons. Wrapping around this is the hadronic tile calorimeter section. At the ends of the detector are further calorimeter sections, the end-caps: one for EM particles and one for the hadronic. Inside the end-caps is a final combined calorimeter, called the forward calorimeter, measuring all particle types. The forward calorimeter has poor resolution, as it only catches a small part of each jet, and is intended more as a means to quantify missing energy.

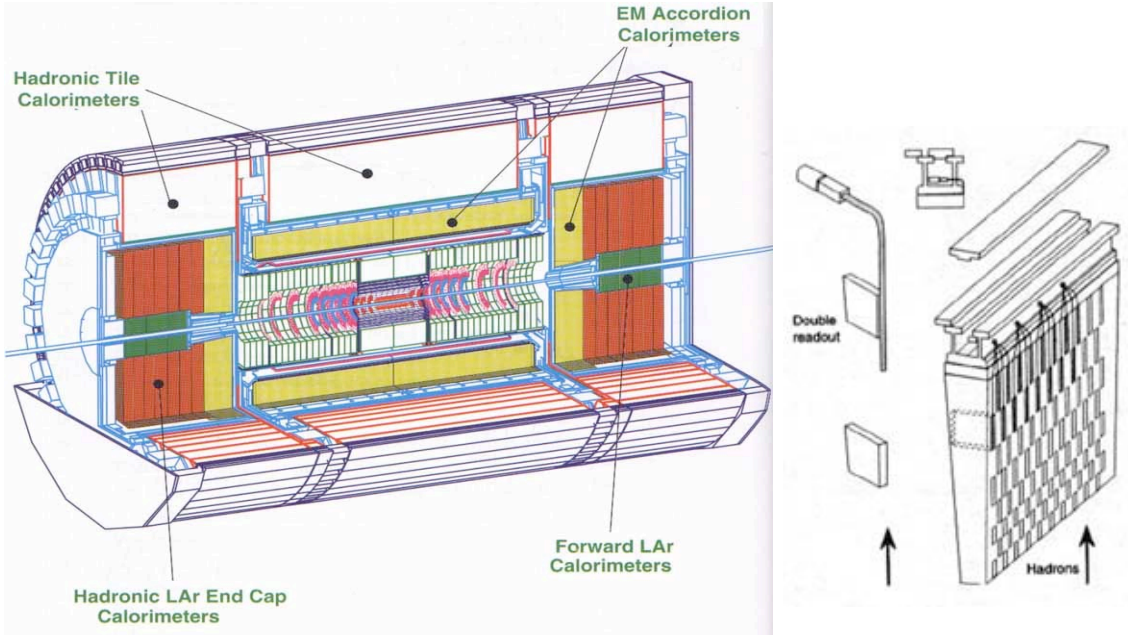


Figure 1: Left, ATLAS calorimeters. Right, detail of hadronic tile-cal section. Notice the sandwiching of the scintillator. Reproduced from [6].

As a particle enters the calorimeter it interacts with the matter inside producing yet more particles, but with less energy. Electromagnetic particles interact and deposit their energy quickly enough to be fully measured within the confines of the electromagnetic calorimeter alone. Hadrons however travel much further, and thus need additional calorimetry to fully measure the energy. Some of their energy does actually get deposited as they travel through the electromagnetic calorimeter. Also, for jets, some of the particles in the jets can themselves be electromagnetic particles. Because of these

two facts, on average approximately 50% of the energy of a jet is actually measured by the electromagnetic calorimeter, even though the jet forms from a strongly interacting particle. The fact that jet energy is measured by two different calorimeters leads to an effect called non-compensation (discussed later under sources of nonlinearity).

As previously mentioned the hadronic calorimeter is made up of two types of detectors, a tiled iron-scintillator barrel region and the end-cap that uses liquid argon [1]. It is divided into around 5000 cells readout on 10000 channels and covering the full azimuth around the beam interaction point and up to ± 3.2 in rapidity¹. The calorimeter is three cells deep with each cell occupying $\sim 0.1 \times 0.1$ in rapidity and azimuth. A stack of three cells (all with the same η & ϕ) is called a tower. The tiled iron-scintillator calorimeter is assembled into three separable wheels: the main barrel covers $|\eta| < 1.0$ and extended barrels either side continue coverage for $0.8 < |\eta| < 1.7$. From $1.0 < |\eta| < 1.6$ reduced coverage exists due to gaps needed for electronic and cryogenic access. This leads to a decreased resolution in the region. The hadronic liquid argon end-cap calorimeter extends coverage up to $|\eta| < 3.2$.

Sources of Non-linearity in the Energy Measurement

An ideal instrument or measuring tool should have the property that doubling the input also doubles the value returned by the measuring device; that is, it should be linear in response. With the hadronic calorimeter, however, many unavoidable circumstances affect it in a way that makes the response non-linear. In order to make a useful measurement with the detector, it must be calibrated for many values extending over the full range of desired detection; in this case a few GeV up to several TeV.

Possibly the greatest source of non-linearity in the energy reconstruction comes from dead matter in the detector, that is material not involved in energy measurement. This can include the magnet system, cryostats, electronics for read-out, and supports holding each of the various sub-detectors in position. As mentioned in the introduction, some of this dead matter is positioned between the main and extended barrels of the calorimeter, and affects any jet entering that portion of the calorimeter. Still more dead matter resides in front of the hadronic calorimeter, between it and the EM calorimeter. The variation in dead matter in both azimuth and rapidity mean that the calibration must be done for every cell in the calorimeter, and cannot be inferred from a single set of cells.

Another often-touted non-linear effect is known as non-compensation. Jets, while arising mainly from strongly interacting particles (quarks and gluons) can contain in them electromagnetically interacting particles due to decay of parent bodies in the jet. For example a π^0 decays quickly into two photons. This part of the jet is measured in electromagnetic calorimeter. The jet energy is reconstructed from a combination of the measured energy deposit in both calorimeters. However, the responses of the two calorimeters are not the same. Thus, a jet composed of many electromagnetic particles will have a different reconstructed energy than one with only hadronic particles even if the actual energies of the two jets are the same. This effect therefore affects the resolution of the detector as a whole for measuring jet energies. Non-compensation is expected to contribute a constant term of 3% to the energy resolution [2].

¹ rapidity: Useful variable for parameterization in high energy physics. $\eta \equiv -\ln(\tan(\theta/2))$ where θ is measured from the beam line. Therefore, $\eta = 3.2$ corresponds to an angle of inclination of 5° .

Other, smaller effects will also sum to produce noticeable non-linearities. The finite size of the detector means that some energy can escape out of the back of the detector. This leakage, while small (about 2% at 100 GeV) [1], increases logarithmically with energy.

Sensitivity of Physics Studies to Miscalibration

To illustrate the need for detailed full range calibration we can consider the effect of calibration uncertainties on a physical study such as quark compositeness. Quark compositeness is the idea that quarks themselves are composed of yet smaller particles, called preons. The ground state of a preon pair or trio would then be the lowest energy quarks – up and down – and excited states of the preons the higher energy quarks: charm, strange, top and bottom. While a complete theory for preon interactions has yet to be formulated, it has been shown [3] that compositeness would cause a change in the cross-section of quark-quark hard scattering due to the additional interaction term. This term (see equation 1) would depend on a scaling constant Λ describing the strength of the preon-preon interaction.

$$\text{Equation 1: } \frac{d\sigma(q_i q_j \rightarrow q_i q_j)}{dz} = \text{Standard Model} + \frac{\pi}{2s} \left(\frac{s^2}{\Lambda^4} \right)$$

A study by Z.U. Usubov [4] explores the sensitivity of ATLAS in detecting compositeness. Two of the more pertinent plots are reproduced here for illustration. Plots below show the resulting P_t distribution for 30 fb^{-1} data (expected in the first few years of running). The first plot shows P_t distributions including the standard model (no compositeness) and compositeness models up to 25 TeV. A second plot gives the fractional deviation of the compositeness signals from the standard model. All data was produced with ATLFAST [5], a fast algorithm for event creation and reconstruction (see conclusion for discussion of ATLFAST).

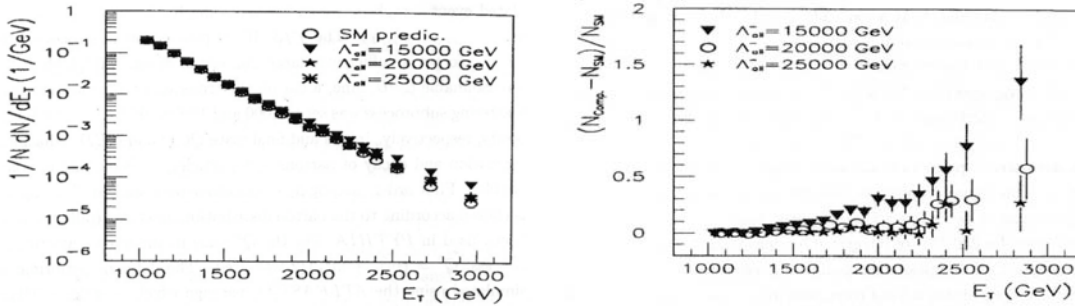


Figure 2: Signal for quark compositeness at ATLAS, QCD hard-scattering cross-section (simulated by ATLFAST). Plots are for 30 fb^{-1} of data. The Standard Model as well as different compositeness scales are shown. Left, a) is the distribution as a function of transverse momentum of the jets. Right, b), shows the deviation from the standard model of the distributions. Reproduced from [4].

Usubov also introduces a residual non-linearity to see how the data would be affected. This non-linear term added to the reconstructed energy is ad hoc, but could be considered similar to energy lost out of the back of the detector (proportional to the log of the energy of the jet). By comparing the above plot 2b), we can see such a non-linearity could mask a quark-compositeness by shifting the data back towards the standard model curve. Similarly, a mis-calibration in the other direction could produce a false compositeness signal.

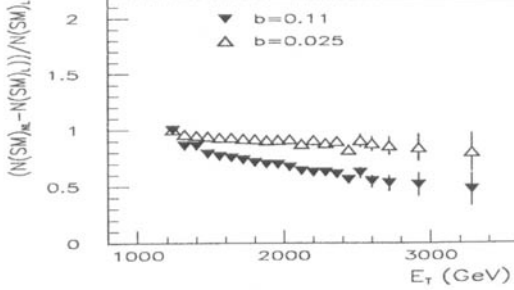


Figure 3: QCD hard-scattering distribution with non-linearities normalized to the linear distribution. Two scales of non-linearity are shown. Reproduced from [4].

Calibration Schemes

Before discussing the details of the individual calibration methods, it is good to recall some simple facts about statistical measurements and apply them to the calibration of the hadronic calorimeter. In general for N measurements we can consider the mean value of the measurement, the standard deviation of the measurement, and the standard deviation of the mean itself (SDOM) defined by:

$$\text{Equation 2: } \frac{\sigma_{\text{mean}}}{E} = \frac{1}{\sqrt{N}} \frac{\sigma_{\text{measuement}}}{E}$$

In the context of calorimeter calibration the standard deviation is the resolution of the detector and the SDOM is the uncertainty in calibration. In most cases $\sigma_{\text{measuement}}$ is dominated by the resolution of the hadronic calorimeter itself. The hadronic calorimeter resolution has been measured in test bed studies and is given by:

$$\text{Equation 3: } \frac{\sigma_{\text{Hcal}}}{E} = \frac{50\% \sqrt{\text{GeV}}}{\sqrt{E}} + 3\%$$

Thus, at $E = 200$ GeV, for a desired uncertainty in the calibration of 1%, we need ~ 40 events, and at 1 TeV ~ 20 . We would like to calibrate each cell individually, but to increase the reach of the calibration we can sum the statistics over azimuth taking advantage of the high degree of azimuthal symmetry in the detector. The rest of this paper is devoted to exploring the reach of the statistics for various calibration schemes in calibrating the hadronic detector.

To obtain this calibration a number of methods will be employed. Some initial calibration is done on the test beam setup using beams of pions or protons produced by the SPS at CERN. This can produce beams with energies up to 400 GeV. Once the detector is assembled a radioactive Cs^{137} source sent through special calibration holes drilled in to the cells can then be used to inter-calibrate all the remaining cells with those calibrated on the test beam setup. This method, while calibrating the energy readings of individual cells, does not account for larger effects on energy measurement due to dead matter, leakage, and saturation. Also, since the SPS is limited to 400 GeV beams, the calibration at higher energies is not known. Furthermore, more subtle differences between the *in situ* performance and the test beam measurements (such as extraneous fields and temperature gradients across the detector) need to be studied and accounted for in the final calibration. Therefore, *in situ* calibration schemes are also needed.

One such method takes advantage of the fact that the energy of relativistic particles is almost precisely equal to their momentum ($E/p - 1 < 10^{-3}$ for $E > 10 \text{ GeV}$) [6]. Then, the calorimeter can be calibrated using the tracker, which can infer the momentum of the particle from its track curvature. This is the primary means to calibrate the electromagnetic calorimeter using electron/positrons. The technique is more difficult with the hadronic calorimeter since it is difficult to trigger on single isolated hadrons. Studies have been presented for such a method, however [7]. At higher energies, the calibration error is dominated by the error in the momentum measurement, which increases linearly with energy [8].

Still other techniques for calibration use particle resonances to calibrate. The best known is the Z_0 resonance at 90 GeV. Most of the decays are to two jets entering into the hadronic calorimeter. The draw back of such calibration is that it really only allows for a single calibration point; in the case of Z_0 calibration we have two back-to-back jets with $P_t = 45 \text{ GeV}$. $Z_0 Z_0$ decays and initial state radiation² allow for initial $P_t \neq 0$ that can thus calibrate to higher energies, however these types of events occur much less frequently and thus have poor statistics.

γ -Jet calibration

Another calibration method uses measurements made by the electromagnetic calorimeter to calibrate those made using the hadronic calorimeter. This is done using events that produce particles measured in both regions, namely photon + jet events. As mentioned in the introduction, photons lose their energy to the calorimeter in a simple, straightforward way. The energy measured therefore is known very well (with good resolution). Also, there is less dead matter in front of the EM calorimeter, and there is no non-compensation effect (EM particles are measured entirely within the EM calorimeter). These facts together mean that the EM calorimeter will be much easier to calibrate than the hadronic. Events that produce one EM particle and one hadronic particle can be used to transfer this calibration over to the hadronic calorimeter.

² Initial State Radiation: Particles emitted from the proton prior to the pp collision. Can cause a nonzero initial transverse component to the momentum.

The transfer is done by a simple fact about the geometry of the collisions. Recall that the initial collision is between one quark or gluon in each of the protons. Due to energy sharing inside the proton, the two colliding quarks or gluons will not necessarily have the same momentum, and thus the final direction and energy of the outgoing particles may not balance.

However, it is true the transverse component of the initial collisions is always zero (the protons collide head-on). Conservation will require the outgoing particles to balance their transverse momentum. Thus, instead of discussing the full energy of particles, we consider their transverse component (P_t) instead.

The γ -jet calibration method has been studied in detail in the case of the CMS detector [9]. Assuming 10fb^{-1} of data, the method should allow for an absolute energy calibration up to 650 GeV. Figure 5 shows the distribution of the data into cells in the calorimeter. Shown are both the P_t component and total energy of the jet entering the calorimeter. Data is binned 50 GeV per bin, 0.1 in rapidity. The plot is integrated over azimuth. In the range of $0 < P_t < 300$ GeV statistics are good enough for calibration of cells individually. The calibration can be extended up to 650 GeV by averaging over azimuth. Thus we obtain calibration of jets with P_t up to 650 GeV in the region $|\eta| < 1$ or $300 \text{ GeV} < P_t < 650 \text{ GeV}$ $1 < |\eta| < 3.2$.

Figure 4: Collision geometry and P_t balancing.

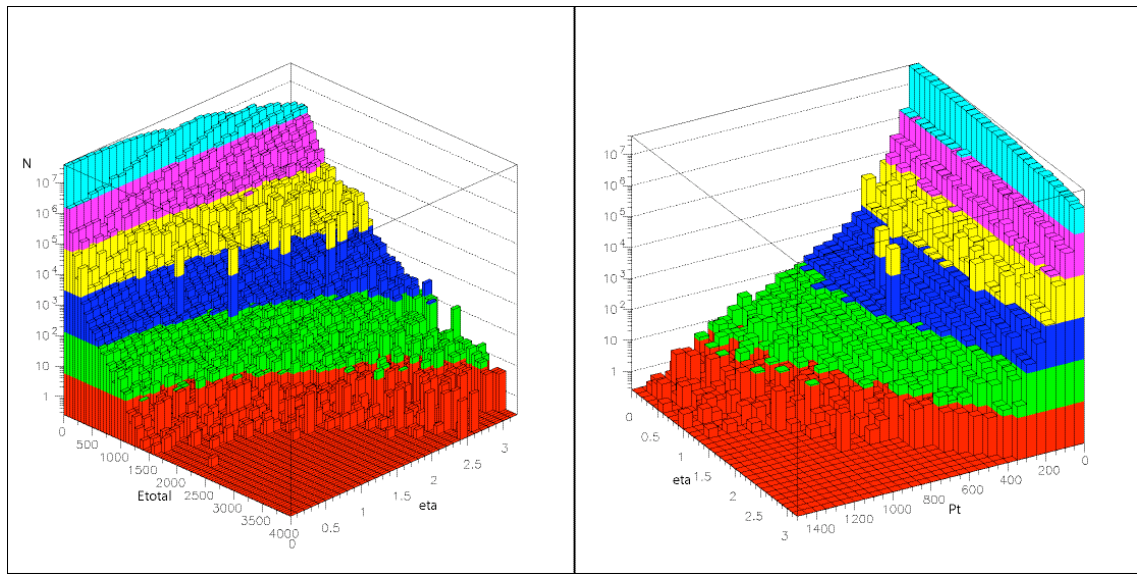


Figure 5: Population of ATLAS hadronic calorimeter by γ -jet events. 10 fb^{-1} data assumed. a) Left is the P_t distribution, b) right the full energy. Data is integrated over ϕ .

The coverage can be extended somewhat using QCD hard scatter dijet events that have one jet in the calibrated region and the other out at higher rapidity. A jet with $400 < P_t < 650$ and $|\eta| < 1$ can be said to be calibrated based on the previous calibration using γ -jet events. Using P_t balance regions not reached by the γ -jet events are calibrated instead using the dijet data. Figure 6 shows the additional coverage using this method.

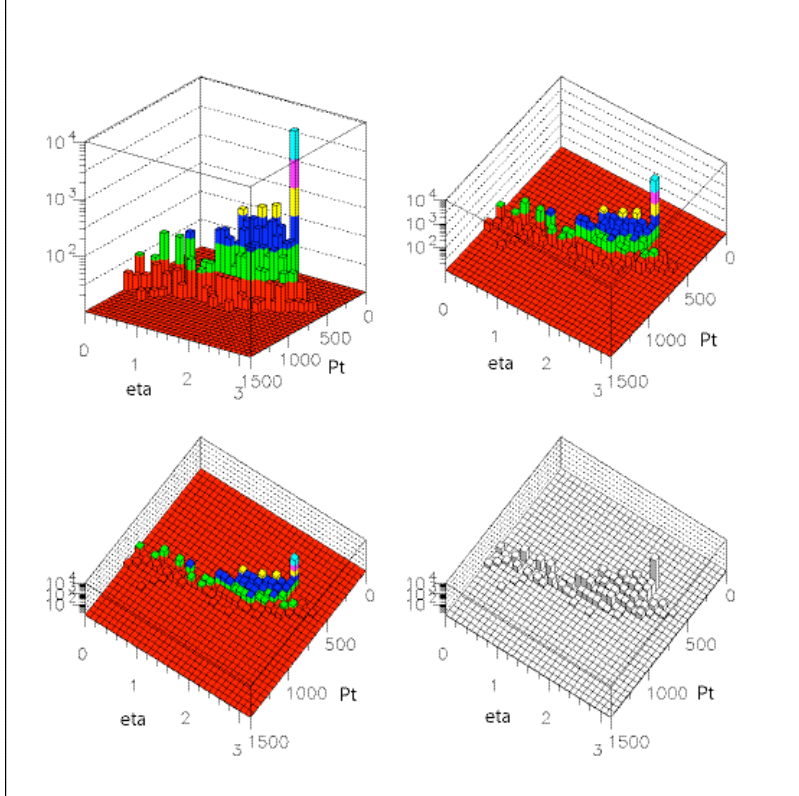


Figure 6: Additional coverage from dijet events. Cuts on the dijet data sample put one jet in a region of the calorimeter calibrated by the γ -jet events. The other is used to calibrate a new region of $P_t - \eta$ using P_t balance between jets.

Multi-Jet Calibration

QCD hard scattering events can actually help us much further. While dijet events are the most common final state of a quark-gluon or similar scattering, some events actually result in three or more jets due to the partonization process. For instance, if a scattered gluon decays into a quark and antiquark heading in opposite directions (in their rest frame) each of those could then form separate jets. For the overall event then there would be three jets: one large and two smaller jets with $P_t \sim 1/2$ that of the larger jet. We can use such events in a similar manner as discussed with the dijet extension, to extend the calibration not just to higher rapidities, but also to higher ranges of P_t . The γ -jet calibration will give us certainty in the absolute energy calibration up to 650 GeV in the main barrel. Events with two or more jets with $P_t < 650$ GeV can then be used to calibrate another jet in the event with $P_t \sim 1$ TeV. Equation two gives the modified P_t balancing scheme needed. Given $P_{t,1}$ = jet with largest P_t (the jet we want to calibrate for):

$$\text{Equation 4: } P_{t,1} + \sum P_{t,i} \cos(\phi_i - \phi_1) = 0$$

The statistics for this calibration scheme were again studied using ATLFEST. The numbers and plots discussed are for 10 fb^{-1} of data. Cuts were made on the second and third largest jets in the event, requiring the second largest to have $P_t < 0.6 P_{t,\text{largest jet}}$. The third jet had a cut for $P_t > 0.2 P_{t,\text{largest jet}}$ although this cut was actually implicit in the first cut and made no change. Further cuts make sure the jets were separate (to avoid double counting cell energies and to make sure the multiple jets weren't a matter of poor jet definition in the reconstruction) by requiring their jet centers to be separated by more than 0.6 in eta-phi.

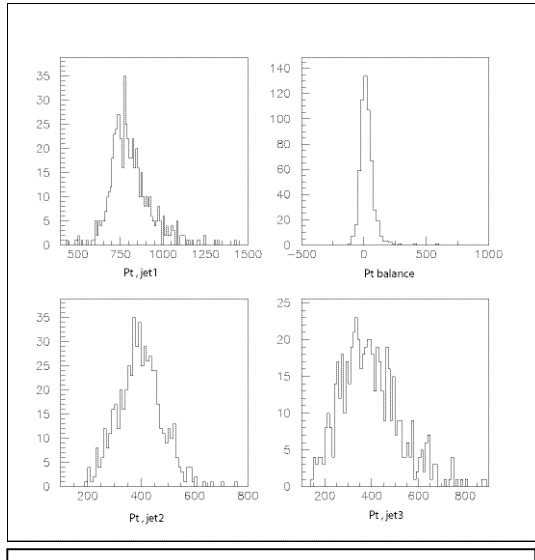


Figure 7: Description of multi-jet QCD hard-scattering events.

The plot left shows the effectiveness of cuts on a data sample of 20000 events with $750 < P_t < 1000 \text{ GeV}$ as set in Pythia (reconstruction spreads this range). The number of events after cuts is ~ 700 , or 4% of the total QCD hard-scatter events. While this is a small fraction, the very large overall statistics for QCD hard-scattering easily balances this and we obtain good statistics up to around 1 TeV as shown by the next two plots. Figure 8a shows the population of the calorimeter by the multi-jet events, summed over azimuth. Figure 8b is the same data summed also over rapidity and makes clearer the reach of the calibration. Recalling the statistics criteria for jets falling into a single cell we can expect obtain a full absolute energy calibration for jets up to 1.1 TeV.

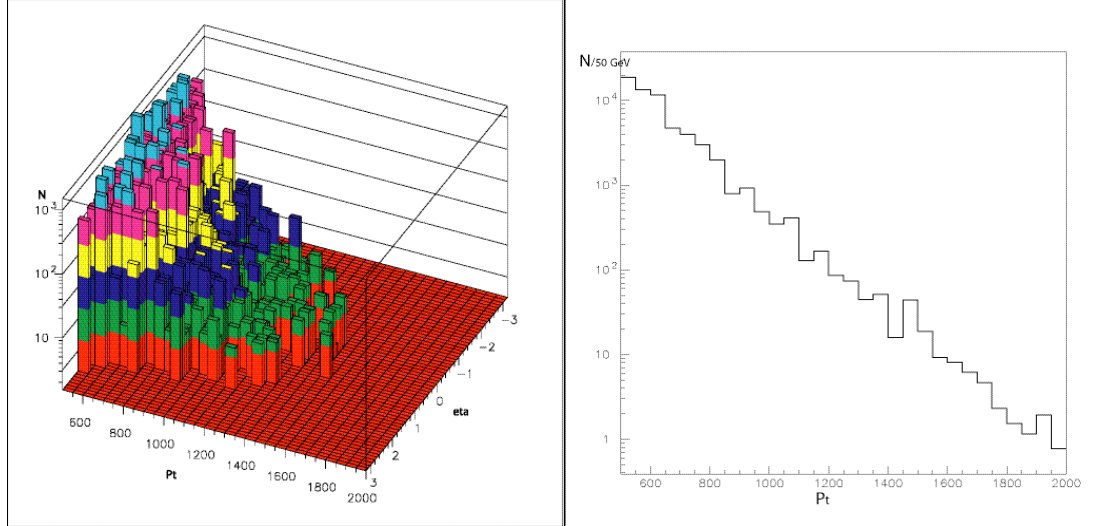


Figure 8: Population of calorimeter by QCD hard-scatter, multi-jet events. 10 fb^{-1} data. Left a) Distribution of both P_t and η , right b) P_t only (summed over η and ϕ).

Conclusion

Throughout the paper the ATLAS detector response was simulated using ATLFAST. This program ports using the Athena framework to the event generators Pythia and Jetset, and to algorithms for energy reconstruction. A vast amount of detail of the real detector is lost in this reconstruction; there is only one generalized calorimeter, no dead matter or energy leakage is simulated. Interactions inside the calorimeter are not simulated; instead the full energies of the particles produce from partonization of the initial quark or gluon are dumped into ATLFAST cells. These ‘cells’ resemble more a tower in the real detector than individual cells, that is, there is no depth sampling in ATLFAST. During jet reconstruction a smearing function is applied to obtain a resolution matching that found in test beam studies.

Still, ATLFAST does allow a quick, easy quantification of the statistics available for various physics studies, in this case absolute energy calibration. In the first year of running of the LHC we expect that, using a combination of physics processes, an absolute energy calibration up to 1.1 TeV (<1% uncertainty) can be achieved in the region of $|\eta| < 1.0$. If we sum the statistics over azimuth (& assign the same calibration to those cells) we can extend the calibration to $1.3 \text{ TeV} \pm 50 \text{ GeV}$. This combination should include, though not exclusively, γ -jet events as well as multi-jet QCD hard-scattering events. Further studies using GEANT should still be performed to quantify expected residual non-linearities after calibration.

Acknowledgements

I would like to thank Frank Merritt and Ed Blucher for their useful discussions over my research. Also thanks go to Peter Sherwood and Elzebita Richter-Was for help with ATLFAST. Of course I owe much also to my advisor James Pilcher. Last I would like to thank the physics department and the University of Chicago as a whole for a great education and a wonderful four years.

Sources

1. ATLAS, Tile Calorimeter Technical Design Report, ATLAS TDR 3, CERN/LHCC 96-42, (1996).
2. M. Bosman, Y. Kulchitsky, M. Nessi. ATLAS Internal Note. ATL-TILECAL-2000-002. (2000).
3. E. Eichten, K. Lane and M. Peskin. Phys. Rev. Lett. 50, 811 (1983).
E. Eichten et al., Rev. Mod. Phys. 56, 579 (1984).
4. Z.U. Usibov. Phys. At. Nucl. 64, no.2, 332. (2001).
5. E. Richter-Was, D. Froidevaux and L. Poggioli, ATLAS Internal Note, ATL-PHYS-98-131 (1998)
6. ATLAS, Calorimeter Performance Technical Design Report, ATLAS TDR 1, CERN/LHCC 96-40, (1996).
7. H. Plothow-Besch. ATLAS Internal Note. PHYS-No-067 (1995).
8. ATLAS, Inner Detector Technical Design Report, ATLAS TDR 4, CERN/LHCC 97-16, (1997).
9. D.V. Bandourin, V.F. Konoplyanikov, N.B. Skachkov. JINR E2-2000-251 (2000).